Available online at www.sciencedirect.com
SCIENCE DIRECT
Journal of Catalysis 232 (2005) 456–466
JOURNAL OF CATALYSIS
www.elsevier.com/locate/jcat

Mechanism of butane skeletal isomerization on sulfated zirconia

Xuebing Li, Katsutoshi Nagaoka [1], Laurent J. Simon [2], Roberta Olindo, Johannes A. Lercher *

Department of Chemistry, Technische Universität München, Lehrstuhl für Technische Chemie II, Lichtenbergstraße 4, 85747 Garching, Germany

Received 14 December 2004; revised 8 March 2005; accepted 31 March 2005

Available online 10 May 2005

Abstract

A kinetic model of the skeletal isomerization of *n*-butane and isobutane on sulfated zirconia in the absence of Pt is presented. The skeletal isomerization of butane on sulfated zirconia has been shown to be initiated by oxidative dehydrogenation of the alkane. This is followed by the formation of alkoxy groups/carbenium ions at the surface, induced by strong Brønsted acid sites. The isomerization of the *sec*-butyl carbenium ion occurs mono-molecularly, as suggested by the 100% selectivity for isomerization extrapolated to zero conversion. With increasing conversion, the selectivity decreased linearly, leading to propane and pentanes up to 40% of conversion. The lower selectivity for isomerization is qualitatively explained by reactions of isobutene present in small concentrations in the reactor at higher conversions. Transient experiments show conclusively that the isomerization of the carbenium ion and not the hydride transfer from the alkane to the carbenium ion is the rate-determining step.

Keywords: Sulfated zirconia; Butane; Isomerization; Kinetics; Hydride transfer; Chain propagation; Activation energy

1. Introduction

Sulfated zirconia and other sulfated metal oxides are of interest because of their unique activity for skeletal isomerization of short alkanes at low temperatures [1,2]. In recent years the kinetics of butane isomerization on sulfated zirconia has been studied frequently [3–7], and the results have been reviewed [8]. However, the marked differences in *n*-butane and isobutane isomerization reactions indicate that the conclusions reached for a narrow set of conditions may not be generalized.

An induction period is observed, when butane is isomerized on sulfated zirconia at low temperature, which is assumed to be due to the accumulation of carbenium ion species on the surface [9,10]. The presence of butenes shortened the induction period significantly [11], which is rationalized by the easier formation of carbenium ions by protonation. The importance of carbenium ions during alkane skeletal isomerization on sulfated zirconia has also been indicated by the negative effect of CO (formation of oxocarbenium ion) [9,12]. Quantum chemical studies have contributed significantly to the understanding of the state of these carbenium ions and their conversion [13].

Intermolecular (bimolecular, involving a *sec*- or *tert*-octylcarbenium ion) and intramolecular (monomolecular) routes [14–21] have been proposed for butane isomerization on solid acids. The intramolecular isomerization of a butyl carbenium ion requires the formation of a primary carbenium ion, which is characterized by a high-energy barrier in the gas phase. Therefore, the intermolecular mechanism was speculated to be the preferred route, as it involves only the formation of secondary carbenium ions, followed by cracking and the subsequent hydride transfer/desorption step. In this context, it should be noted that the kinetics of *n*-butane isomerization was analyzed previously with the assumption that dimerization and cracking are involved [3]. The high isobutane selectivity (90–92%) during *n*-butane isomeriza-

* Corresponding author. Fax: +49 89 289 13544.
E-mail address: johannes.lercher@ch.tum.de (J.A. Lercher).
[1] Present address: Department of Applied Chemistry, Faculty of Engineering, Oita University Dannoharu 700, Oita 870-1192, Japan.
[2] Present address: IFP-Lyon, Catalysis and Separation Department, BP-3, 69390 Vernaison, France.

0021-9517/$ – see front matter © 2005 Published by Elsevier Inc.
doi:10.1016/j.jcat.2005.03.025

tion was explained by the different stability and reactivity of the C_8 isomers, and the low reaction rate of isobutane was ascribed to the steric hindrance of two *tert*-butyl groups forming the C_8 intermediate.

n-Butane isomerization carried out in the presence of hydrogen showed a reaction order for *n*-butane above 1 [4]. Therefore, the intermolecular mechanism was concluded to dominate under these conditions. The opposite conclusion was reached by Garin et al., who used mono ^{13}C-labeled *n*-butane under similar reaction conditions [16]. However, in most of the experimental works dealing with isomerization of ^{13}C-labeled *n*-butane on promoted and unpromoted sulfated zirconia at low temperature, an extensive isotopic scrambling was observed. These results were used as evidence for an exclusive or prevailing bimolecular route [4,15,18,20,22]. It should be noted that in all of these papers either the concentration of olefins in butane was not specified and/or a purification step was not documented. In addition, the reported conversion at which the reaction mixture was analyzed for isotopic scrambling was much higher than that corresponding to differential conditions (for example, 40% in Ref. [15] and 10% in Ref. [18]). It is important to note that the results of Garin (in favor of a monomolecular mechanism) were critically reinterpreted by Adeeva et al. [8], who stated that the absence of isotope scrambling does not prove the mechanism to be intramolecular.

The complete absence of disproportionation products, propane and pentanes, at least in the early stages of *n*-butane isomerization on sulfated zirconia [14] or other acid solid catalysts [21], has been interpreted as evidence for a monomolecular mechanism. However, results of Luzgin et al. suggested that at lower conversions intermolecular pathways to isobutane are conceivable. In this context it should be noted that the cracking products of branched octanes on sulfated zirconia at 373 K do not lead exclusively to isobutene, and hence octylcarbenium ions were concluded not to be the main intermediates of butane isomerization [23].

In summary, the experiments reported here do not allow us to unequivocally decide the pathways along which *n*-butane skeletal isomerization proceeds. This is among other factors to be ascribed to impure feeds, which induce various reactions, including oligomerization and deactivation. After having demonstrated that the initiation step consists of the oxidative dehydrogenation of *n*-butane [10], here the propagation step of the butane skeletal reaction on sulfated zirconia at 373 K is addressed.

2. Experimental

2.1. Catalyst preparation

Sulfate-doped zirconium hydroxide was obtained from Magnesium Electron, Inc. (batch number XZO 1077/01). The as-received sample was heated to 873 K with an increment of 10 K/min and maintained at the final temperature for 3 h in static air to form sulfated zirconia with a concentration 0.053 mmol/g of Brønsted acid sites. The resulting catalyst was kept in a desiccator and was activated in situ as described below before the kinetic studies.

2.2. Adsorption isotherms and differential heats of adsorption

The adsorption isotherms were measured in a SETARAM TG-DSC 111 instrument. Approximately 15 mg of pellets was charged into the quartz crucible used in the TG-DSC system. The sample was activated by heating to 673 K with an increment of 10 K/min and maintained at 673 K for 2 h in vacuum ($p < 10^{-6}$ mbar). After activation, the temperature was stabilized at 373 K. *n*-Butane and isobutane were introduced into the closed system in small doses and allowed to equilibrate with the sulfated zirconia until no further mass increase was observed. The butane pulses were repeated until the pressure reached 300 mbar. The differential heats of *n*-butane and isobutane adsorption were determined at 308 K.

2.3. Butane isomerization

Isomerization of *n*-butane (99.5%, Messer) and isobutane (99.95%, Messer) was carried out in a quartz micro tube reactor (8 mm i.d.) at atmospheric pressure under differential conditions (conversion $< 0.5\%$). Sulfated zirconia pellets (355–710 μm) (0.2 or 0.5 g for *n*-butane or isobutane, respectively) were loaded into the reactor and activated in situ at 673 K for 2 h in He flow (10 ml/min). The catalyst was cooled to 373 K, and the reactant mixture (various *n*- and isobutane partial pressures in He, total flow of 20 ml/min) was passed through the catalyst bed. Butane was passed through an olefin trap containing activated zeolite H-Y (20 g), before it was mixed with He. The butene concentration in the resulting gas was below the detection limit (i.e., < 1 ppm). The reaction products were analyzed with an on-line HP 5890 gas chromatograph (GC) equipped with a capillary column (Plot Al_2O_3, 50 m × 0.32 mm × 0.52 mm) connected to a flame ionization detector (FID).

In order to investigate the catalytic activity and selectivity of sulfated zirconia for *n*-butane (5% *n*-butane in He) at high conversion, 1.5 g of sulfated zirconia was loaded into the reactor, and reactant flow rates between 0.5 and 2 ml/min were applied.

2.4. Transient kinetic analysis

A concentration transient study during *n*-butane isomerization at 373 K (0.2 g of sulfated zirconia, 20 ml/min of 5% *n*-butane in He) on sulfated zirconia was performed after 5 h TOS (time on stream), when stable activity was observed. The feed was changed in a step function from 5 vol% *n*-butane to 2 vol% propane in He or pure He (20 ml/min). Samples of the effluent were collected with a VICI 32-port valve (16 loops) and analyzed by GC.

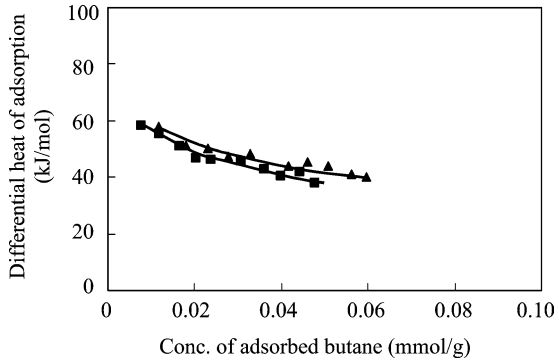

Fig. 1. Differential adsorption heats of (▲) *n*-butane and (■) isobutane adsorption at 308 K on sulfated zirconia (activated in vacuum at 673 K for 2 h).

3. Results and interpretation

3.1. Differential heats of butane adsorption

The differential heats of *n*-butane and isobutane adsorption as a function of the butane coverage determined at 308 K are compiled in Fig. 1. For *n*- and isobutanes, the heats of adsorption depended similarly on the coverage, starting at approximately 60 kJ/mol (at low coverage) and declining to about 40 kJ/mol at 40 µmol/g coverage. Thus, overall, two isotherms (adsorption sites) seem to coexist, which may include chemisorbed butane molecules at low pressures.

3.2. n-Butane and isobutane reactions at various partial pressures

The isomer formation rates versus time on stream (TOS) during butane skeletal isomerization on sulfated zirconia at 373 K at various partial pressures are shown in Figs. 2A and 2B for *n*-butane and isobutane isomerization, respectively. All reactions showed an induction period depending in duration upon the butane partial pressure. Higher partial pressure led to a shorter induction period (see Figs. 3A and 3B). After the induction period, the catalyst showed stable catalytic activity with only very slow deactivation.

Because the conversion of butane was lower than 1%, the plug flow reactor is safely concluded to be operated in differential mode, and the reaction rates can also be considered as the intrinsic forward reaction rates. The maximum rate of isobutane formation increased with increasing *n*-butane partial pressure (see Fig. 4A). In addition, the selectivity for isobutane was nearly constant (approximately 96%) at all *n*-butane partial pressures. The main by-products were equimolar amounts of propane and pentanes (*n*- and isopentane at a ratio of 1:4). However, as shown in Fig. 4B, the maximum rate of *n*-butane formation from isobutane increased linearly only for isobutane partial pressures lower than 19 mbar. For higher partial pressures, the isomerization rate increased more gradually, indicating a lower reaction order in isobutane. *n*-Butane formation rates (from isobutane) were about 50 times lower than isobutane formation rates

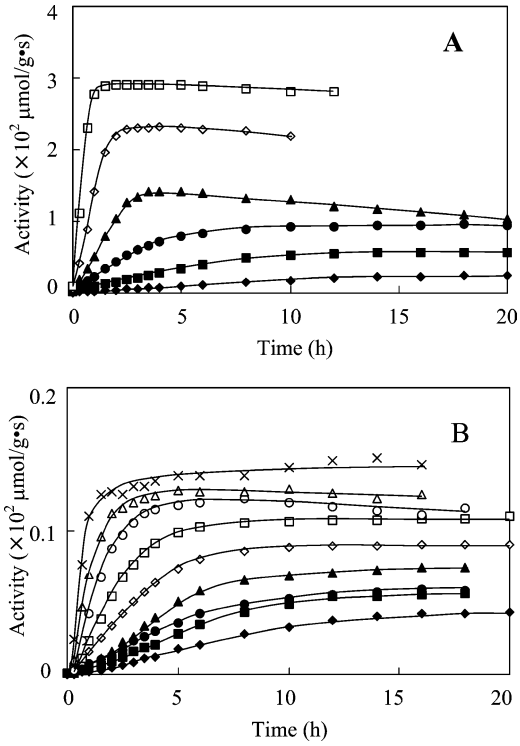

Fig. 2. (A) isobutane formation rates versus time on stream for *n*-butane skeletal isomerization on sulfated zirconia at 373 K for (□) 170, (◇) 100, (▲) 50, (●) 28, (■) 17 and (◆) 7 mbar *n*-butane in the feed; and (B): *n*-butane formation rates versus time on stream for isobutane skeletal isomerization on sulfated zirconia at 373 K for (×) 88, (△) 50, (○) 36, (□) 19, (◇) 13, (▲) 9, (●) 6, (■) 4.6 and (◆) 3.2 mbar isobutane in the feed.

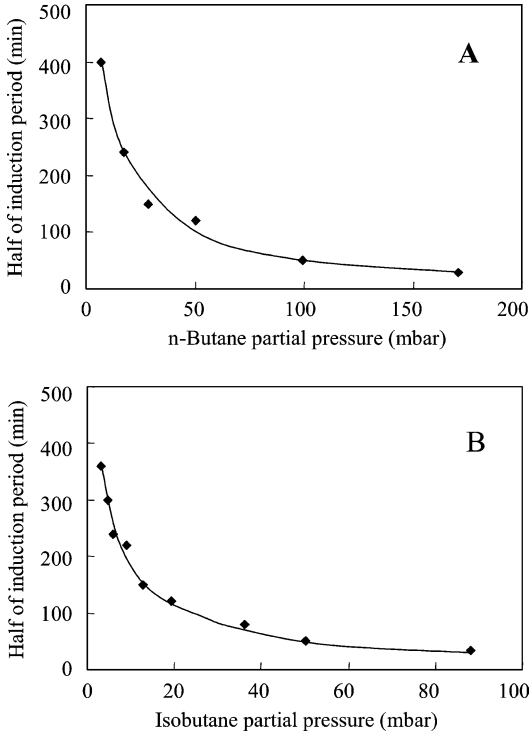

Fig. 3. (A) Half of the induction period versus *n*-butane partial pressure in the feed; and (B) half of the induction period versus isobutane partial pressure in the feed.

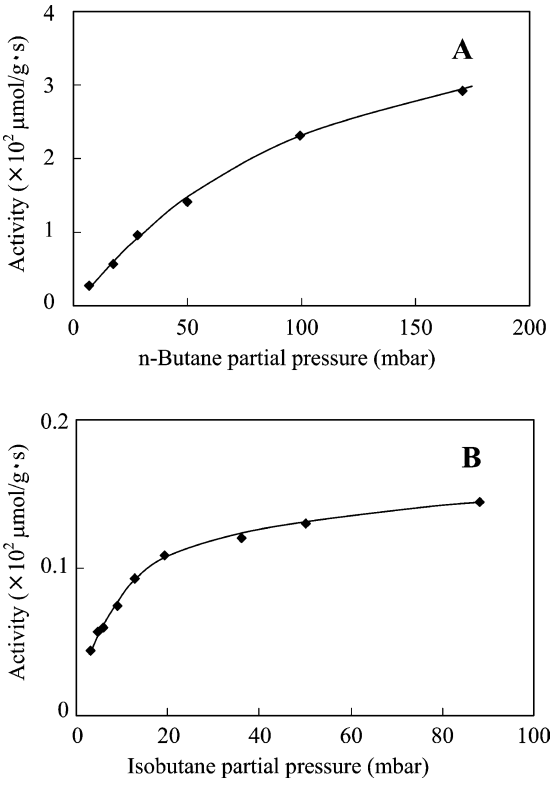

Fig. 4. (A) Experimental isobutane formation rate versus *n*-butane partial pressure; and (B) experimental *n*-butane formation rate versus isobutane partial pressure.

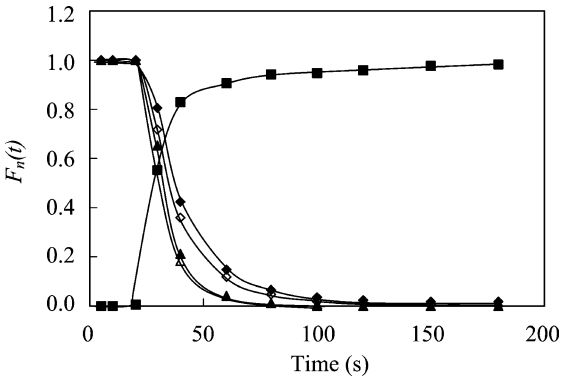

Fig. 5. Normalized transients at 373 K (20 ml/min, 0.2 g_{cat}). (■) Propane, (◇) isobutane, He, (■) isobutane, propane, (△) *n*-butane, He and (▲) *n*-butane, propane.

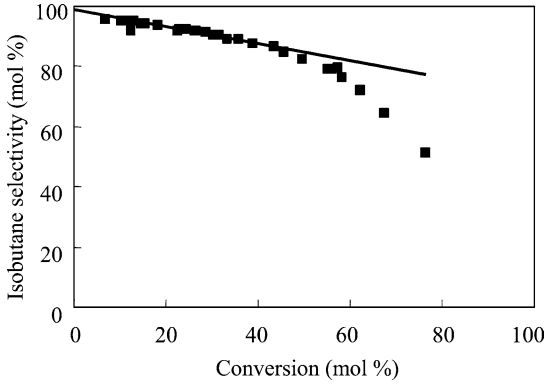

Fig. 6. Isobutane selectivity versus *n*-butane conversion during *n*-butane skeletal isomerization on sulfated zirconia at 373 K.

(from *n*-butane), and the *n*-butane selectivity was approximately 80% at all partial pressures for the former reaction.

3.3. Transient kinetics

Fig. 5 shows the normalized transients $F_{n,i,\mathrm{p}}(t)$ following step change during a transient experiment (where *i* is *n*-butane, isobutane, or propane and p is purge gas, He, or 2 vol% propane in He). When propane is used, *sec*- and *tert*-butyl carbenium ions desorb with hydride transfer from propane, and their concentrations can be determined by integration of the difference in normalized transients during propane and He purge:

$$N_{n\mathrm{C}_4} = C_{n\mathrm{C}_4} \int \left[F_{n,n\mathrm{C}_4,\mathrm{C}_3}(t) - F_{n,n\mathrm{C}_4,\mathrm{He}}(t)\right] \mathrm{d}t.$$

$C_{n\mathrm{C}_4}$ is the concentration of *n*-butane in the product effluent before the start of the transient. The amount of isobutane formed by hydride transfer from propane to *tert*-butyl carbenium ions is also obtained in this way. The results indicate approximately 5×10^{-3} mmol/g of surface *sec*-butyl carbenium ions and only around 3×10^{-5} mmol/g of *tert*-butyl carbenium ions on the catalyst surface at the steady state of *n*-butane isomerization. It should be noted that these concentrations correspond to those at steady state and not to those at thermodynamic equilibrium. The steady-state concentration of *sec*-butyl carbenium ions (5×10^{-6} mol/g) should be compared with the concentration of strong Brønsted acid sites (53×10^{-6} mol/g). Thus 10% of Brønsted acid sites form alkoxy groups at steady state.

Therefore, we conclude that the *sec*-butyl carbenium ion is the dominant species during *n*-butane isomerization, being more than two orders of magnitude higher in concentration than *tert*-butyl carbenium ions. This in turn implies that the rate-determining step has to be the one in the reaction sequence after the most abundant reaction intermediate, that is, the skeletal isomerization of the *sec*-butyl carbenium ion. Note that in case where hydride transfer is the rate-determining step, the most abundant surface species would be *tert*-butyl carbenium ions.

3.4. Product distribution at high conversion

The isobutane selectivity during *n*-butane isomerization on sulfated zirconia at low conversion was approximately 96%. However, as shown in Fig. 6, it decreased with conversion. The decrease was linear at low conversions, and its slope was relatively low up to 60% conversion, whereas above 60% conversion the decline in selectivity was more rapid by far. The isobutane yield increased almost linearly with the conversion up to moderate conversions (approximately 40%), reached the maximum yield at 60% conversion, and decreased at higher conversion (see Fig. 7A). The

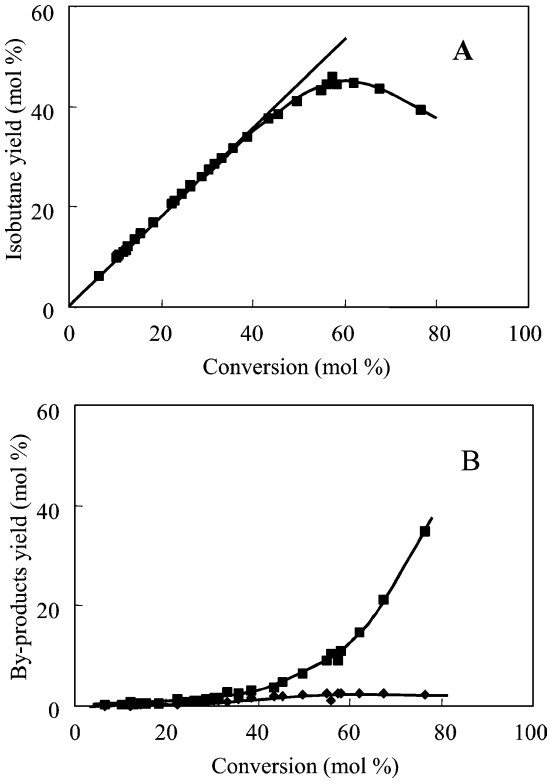

Fig. 7. Yield of products (A) isobutane, (B) (■) propane and (◆) pentanes versus *n*-butane conversion during *n*-butane isomerization on sulfated zirconia at 373 K.

thermodynamic equilibrium value of isobutane at 373 K of 62% [24] was observed at high conversions (80%). In contrast to the kinetically primary product isobutane, the secondary products propane and pentane were formed first in nearly equimolar amounts, whereas at high conversion propane was formed in much larger amounts compared with pentanes (see Fig. 7B).

4. Discussion

4.1. General mechanism at low conversions

The heats of adsorption of *n*- and isobutane on sulfated zirconia and the isotherms are rather similar, leading us to the conclusion that with respect to the principal interaction the two molecules are qualitatively and quantitatively very similar. The moderate decrease in the heat of adsorption suggests a very wide distribution of interaction strength and that the isotherm should be described by a Freundlich or Temkin form.

A minority of the physisorbed molecules are oxidized to butane on the surface [10] and form a *sec*-butoxy group with strong Brønsted acid sites at the surface. The *sec*-butoxy groups (transforming to *sec*-carbenium ions in the transition state) isomerize to *tert*-butoxy groups at the surface and are desorbed via hydride transfer from *n*-butane, forming a new *sec*-butoxy group and isobutane. The principal reaction sequence is depicted in Scheme 1. In the following for simplicity, the term “carbenium ion” is frequently used to describe the stable surface intermediates, but it should be noted that alkoxy groups and not carbenium ions are the stable species in the ground state.

The prevalence of the monomolecular or the bimolecular reaction pathway has been vividly discussed in the literature over a long period without a general consensus being

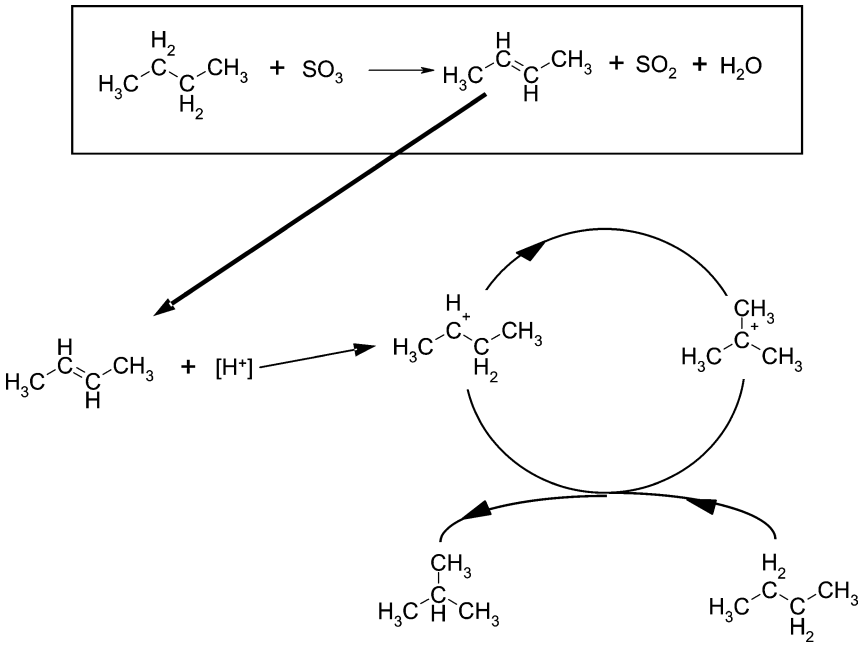

Scheme 1. Proposed *n*-butane isomerization mechanism on sulfated zirconia at low temperature.

reached. This is related in part to the fact that the studies use alkanes with various levels of butene and work under widely differing reaction conditions (up to 150 °C difference in reaction temperature and at various levels of conversion).

In a strict sense, all reaction routes of *n*-butane isomerization proposed involve bimolecular reactions. The different opinions with respect to the mechanisms can be divided into two large groups: (i) those arguing that a *sec*-butyl carbenium ion is isomerized intramolecularly to a *tert*-butyl carbenium ion that desorbs via hydride transfer from a *n*-butane molecule and (ii) those arguing that the *sec*-butyl carbenium ion is alkylated with another olefin, forming a *sec*- or *tert*-octylcarbenium ion, which is isomerized and cracked, forming a smaller olefin, which is re-adsorbed on a Brønsted acid site and finally desorbs, also via hydride transfer from *n*-butane. The relative contributions of the two reaction pathways vary with the concentration of olefins in the reactor, and the conclusions are therefore strongly influenced by the purity of the reactants and the degree of conversion as shown below. However, both reaction schemes depend on the bimolecular step of hydride transfer for chain propagation.

4.2. Direct isomerization of butane versus alkylation/isomerization/cracking route

Without metal components and in the absence of hydrogen in the reactant mixture, sulfated zirconia is a selective isomerization catalyst only at rather low conversions (below 40%). At higher conversion, the isobutane selectivity decreased rapidly, especially when the isobutane concentration in the product was close to the thermodynamic equilibrium concentration (62%). When the relations of yield and conversion (see Fig. 7) are considered, isobutane is clearly a primary product with high stability and a very high ultimate selectivity (close to 100%) at low conversion. Propane and pentane are in turn concluded to be secondary products. If the only reaction pathway were the alkylation/isomerization/cracking route, isobutene, propene, and pentene would be the undetected intermediate products (after readsorption, protonation, and hydride transfer) that should appear as alkane primary products. This clearly suggests that isobutene, propane, and pentane are not formed in a parallel step. As propane and pentane can only be formed via a C_8 intermediate, we conclude that isobutane is formed via an intramolecular route (via methyl cyclopropyl carbonium ions). This argument is supported by other experiments in the literature [14,21]. Note that all labeling studies indicating that an intermolecular mechanism is operative were performed under high conversion [15,20].

Model calculation based on the thermodynamic gas-phase composition for di- and tri-branched octenes led to comparatively low isobutane selectivities. At thermodynamic equilibrium dimethylhexanes are more abundant than trimethylpentanes among the C_8 isomers in the gas phase. Only when it is assumed that on the surface the distribution of C_8 isomers is dramatically changed in favor of 2,2,4-trimethylpentane is it possible to account for a selectivity for isobutane near 100%. However, this scenario seems to be unlikely and it is not supported experimentally. It has been experimentally shown that the cracking pattern of branched octanes at 373 K on sulfated zirconia cannot lead to isobutane selectivity close to 100% as observed with SZ under differential conditions [23].

Theoretical calculations also suggest that the intramolecular skeletal isomerization of butyl carbenium ions is feasible [25]. The activation energy from a *sec*-butyl to a *tert*-butyl carbenium ion has been calculated to be 76 kJ/mol, whereas the activation energy for the reverse reaction, from *tert*-butyl to *sec*-butyl carbenium ion, has been calculated to be 134 kJ/mol. The difference is related to the fact that the *tert*-butyl carbenium ion has a significantly higher stability compared with the *sec*-butyl carbenium ion.

However, the variation in the isobutane selectivity with increasing conversion also indirectly supports the proposed model of an intramolecular isomerization followed by a hydride transfer. The isobutane selectivity decreases at lower conversions linearly with conversion. This decrease indicates that one decisive sequential reaction leading to propane and pentane is first order in the concentration of isobutane. We speculate that this is related to the easier oxidizability of isobutane and hence the higher concentration of isobutene in the gas phase above the catalyst. Furthermore, *tert*-butyl carbenium ions formed in the isomerization process decompose to some extent and may form isobutene. Isobutene reacts with *sec*-butyl carbenium ions to dimethylhexyl alkoxy groups (alkylation reaction), which react as discussed above.

Propane and (to a lesser degree) pentanes are the main by-products during butane isomerization on sulfated zirconia, once it proceeds via the intermolecular dimerization pathway by forming C_8 species from two butyl species followed by rearrangement and cracking. The equal molar amounts of propane and pentane in the product at low *n*-butane conversion in this study are in agreement with previous reports in the literature [3] suggesting the formation and cleavage of octylcarbenium ions with readsorption of the olefins formed and their desorption with hydride transfer from an alkane. However, at high conversion, the yield of pentanes is much lower than that of propane, which suggests that the formed pentenes or pentylcarbenium ions are consumed by further reactions that involve many alkylation and cracking steps. The high selectivity for propane must be related to multiple further cracking and alkylation steps over these catalysts that occur parallel to the isomerization reaction.

The reversible isomerization and the irreversible disproportionation cause the change in selectivity with conversion. At low conversion, the isomerization rate is high and the disproportionation alkylation/cracking proceeds slowly. At high conversion, the integral isomerization rate is lowered as a result of the additional contribution of the isomerization of isobutene, leading finally to a decrease in the isobutane yield above 60% *n*-butane conversion.

4.3. Rate-determining step

The most abundant surface intermediate and in turn the rate-determining step were deduced from a transient experiment analyzing the absolute concentration of *sec*- and *tert*-butoxy groups during *n*-butane isomerization at steady state. We deduced the concentrations by purging the reactor with an inert gas and in the presence of propane as hydride transfer agent. The results show that two orders of magnitude more *sec*- than *tert*-butyl carbenium ions from a catalyst operated at steady state in *n*-butane isomerization could be removed by hydride transfer from propane. The absolute concentration suggests that approximately 10% of all Brønsted acid sites exist in the form of *sec*-butyl alkoxy groups at steady state. The significantly higher abundance of *sec*-butyl carbenium ions demonstrates that the rate-determining step must be in the sequence directly after the formation of the alkoxy groups, that is, the isomerization step. In turn, the result also shows that the hydride transfer step must be in quasi-equilibrium.

In this context it is interesting to note that a quantum chemical study of elementary steps of hydrocarbon transformation in acid zeolite catalysts also suggests a fast hydride transfer step by comparing the relative activation energies, that is, 180–200 kJ/mol for hydride transfer and 257 kJ/mol for *n*-butene to isobutene isomerization [26].

4.4. Description of the initial rate parameters of n-butane and isobutane isomerization

Scheme 2 shows the main reaction steps of the oxidative butane activation and termination and the catalytic cycle of isomerization described in Scheme 1. Step (1) is the irreversible oxidation of *n*-butane to butene, water, and SO_2. The formed butene is protonated by a Brønsted acid site of sulfated zirconia (Step (2)). Step (3) describes the skeletal isomerization of the formed *sec*-butyl alkoxy group/carbenium ion. This step includes the formation of a methyl cyclopropyl carbonium ion, its opening to a primary isobutyl carbenium ion, and its final rearrangement to a tertiary *tert*-butyl carbenium. Step (4) describes the propagation, that is, hydride transfer from *n*-butane to *tert*-butyl carbenium ion with formation of a new *sec*-butyl carbenium ion.

As the concentration of surface *sec*-butyl carbenium ions is more than 100 times higher than that of *tert*-butyl carbenium ions and the surface isomerization has been identified to be the rate-determining step at steady state, the overall rate can be described by the rate equation of Step (3). Because the experiments were performed at very low conversions, only the forward reaction is considered. Thus, the kinetic description is that of the forward reaction only and does not describe eventual butane/butene side reactions at higher temperatures.

Olefins have not been detected in the reaction products and thus are below the 1 ppm detection limit in the GC analysis used. On the other hand, oxidative activation at steady state is slower than that in the induction period but proceeds at a significant rate. Judging by the increase in the concentration of water on the surface, the process should produce sufficient butene to generate a stream of approximately 5 ppm butene in the products [10]. Thus the absence of olefins indicates that at steady state the rate of olefin generation is nearly equal to the rate of its reaction to dead end or side products. This reaction step is fast compared with the generation (Step (1)) but far slower than the olefin protonation and deprotonation. Thus, the concentration of butene can be approximated as constant and below the detection limit in the reactor. Note that in the absence of a termination step the olefin concentration should increase linearly over the catalyst bed (integral reactor treatment).

The initial rate of butane isomerization normalized to the mass of catalyst is therefore described by

$$r_n = k_{n3}[sec\text{-}C_4H_9{}^+].$$

The concentration of the *sec*-butyl carbenium ion can be derived by considering all steps producing and consuming the carbenium ion, whereas the concentration of butene is given by the balance between the oxidative and the terminative step (see Appendix A for the details). Note that at steady state without catalyst deactivation the olefin production is only needed to replace the small loss of olefins by the termination of the acid-catalyzed isomerization cycle. With this approach the initial rate of *n*-butane isomerization is expressed as

$$r_n = \frac{k_{n3} C_B A_n A_n' P_n}{1 + A_n A_n' P_n},$$

where C_B is the concentration of Brønsted acid sites and P_n is the partial pressure of *n*-butane,

$$A_n = \frac{k_{n2}}{k_{n-2} + k_{n3}} \quad \text{and} \quad A_n' = \frac{k_{n1}}{[T]k_{n5}}[SO_3].$$

The rates of isobutane formation obtained from the *n*-butane reaction at various partial pressures are fitted by linearization of the equation. An identical analysis was performed on the isobutane reaction. The values for the composite kinetic parameters are listed in Table 1.

$$n\text{-}C_4H_{10} + SO_3 \overset{k_{n1}}{\rightarrow} n\text{-}C_4H_8 + SO_2 + H_2O \quad (1)$$

$$n\text{-}C_4H_8 + H^+ \underset{k_{n-2}}{\overset{k_{n2}}{\rightleftharpoons}} sec\text{-}C_4H_9{}^+ \quad (2)$$

$$sec\text{-}C_4H_9{}^+ \underset{k_{n-3}}{\overset{k_{n3}}{\rightleftharpoons}} tert\text{-}C_4H_9{}^+ \quad (3)$$

$$tert\text{-}C_4H_9{}^+ + n\text{-}C_4H_{10} \underset{k_{n-4}}{\overset{k_{n4}}{\rightleftharpoons}} i\text{-}C_4H_{10} + sec\text{-}C_4H_9{}^+ \quad (4)$$

$$n\text{-}C_4H_8 + T \overset{k_{n5}}{\rightarrow} n\text{-}C_4H_8\text{–}T \quad (5)$$

Scheme 2. Proposed catalytic cycles for butane skeletal isomerization on sulfated zirconia.

Table 1
Kinetics parameters for butane skeletal isomerization on sulfated zirconia at 373 K

	Rate constant (s^{-1})		Composite constant
k_{n3}	1×10^{-3}	$A_n \times A'_n$	7.7
k_{i3}	2.8×10^{-5}	$A_i \times A'_i$	127

The composite constant for isobutane isomerization ($A_i \times A'_i = 127$) is higher than that for the *n*-butane isomerization ($A_n \times A'_n = 7.7$). Thus, the isobutane reaction rate reaches its maximum at lower partial pressure. The higher constant of the isobutane isomerization can be associated with its higher oxidation reactivity or the higher protonation constant $K_{\text{ipro}} = k_{i2}/k_{i-2}$ of the formed isobutene, because of the higher stability of *tert*-butyl carbenium ion compared with *sec*-butyl carbenium ion.

The isomerization reaction rate constants, k_{n3} and k_{i3}, are 1×10^{-3} s^{-1} and 2.8×10^{-5} s^{-1} for *n*-butane and isobutane isomerization, respectively. More than one order of magnitude difference in the reaction rate constant was found for *n*-butane and isobutane skeletal isomerization. The predicted isomer formation rates of butane skeletal isomerization under differential conditions versus butane partial pressure obtained from our isomerization rate expression and kinetics parameters are also shown in Figs. 8A and 8B for *n*-butane and isobutane, respectively. The model fits the experimental results very well, which indicates that the isomerization reaction of butane can be accurately described by our catalytic cycle and kinetic parameters.

With the rate constants for the rate-determining step, the Gibbs free energy of activation is calculated with the use of transition-state theory:

$$k = \frac{k_B T}{h} \exp\left(-\frac{\Delta G^{0\#}}{RT}\right),$$

where k_B is Boltzmann's constant, h is Planck's constant, and $\Delta G^{0\#}$ is the standard Gibbs free energy of activation. The calculated values of $\Delta G^{0\#}$ were 114 and 125 kJ/mol for the *n*-butane and isobutane isomerization reactions, respectively. The standard enthalpy of activation can be obtained with the equation $\Delta H^{0\#} = \Delta G^{0\#} + T\Delta S^{0\#}$, where $\Delta H^{0\#}$ is the standard enthalpy of activation and $\Delta S^{0\#}$ is the standard entropy of activation. The standard entropy of transition-state species was estimated with the assumption that the transition state is similar to the carbenium ion [27]. Thus, $\Delta S^{0\#} \approx 0$ and $\Delta H^{0\#} = \Delta G^{0\#}$. The true activation energies, obtained from $E_a = \Delta H^{0\#} + RT$, are 117 and 128 kJ/mol for the *n*-butane and isobutane reactions, respectively.

The higher relative activity of the active species formed from *n*-butane, that is, the *sec*-butyl carbenium ion, compared with *tert*-butyl carbenium ion should be related to differences between the ground state and the transition state. Since the *tert*-butyl carbenium ion is the most stable species (that with the lowest potential energy from the molecules and molecular species investigated), the activation energy from the tertiary carbenium ion to the methyl cyclopropyl carbonium ion is higher than that from the *sec*-butyl carbenium ion. However, the activation energy of the *tert*-butyl carbenium ion reaction is only 11 kJ/mol higher than that of the *sec*-butyl carbenium ion. This contrasts with the difference in the free carbenium ions, which is 67 kJ/mol [25]. This is explained by the fact that the carbenium ion in the ground state resembles an alkoxy group more than it does a free carbenium ion [13]. It is even demonstrated that the alkoxides formed in the zeolite frame with primary, secondary, and tertiary carbenium ions have similar potential energies [28]. It is also suggested that with the assistance of the oxygen, the intramolecular skeletal isomerization of butyl carbenium ions is facilitated, providing a lower energy pathway compared with the reaction of free carbenium ions [17].

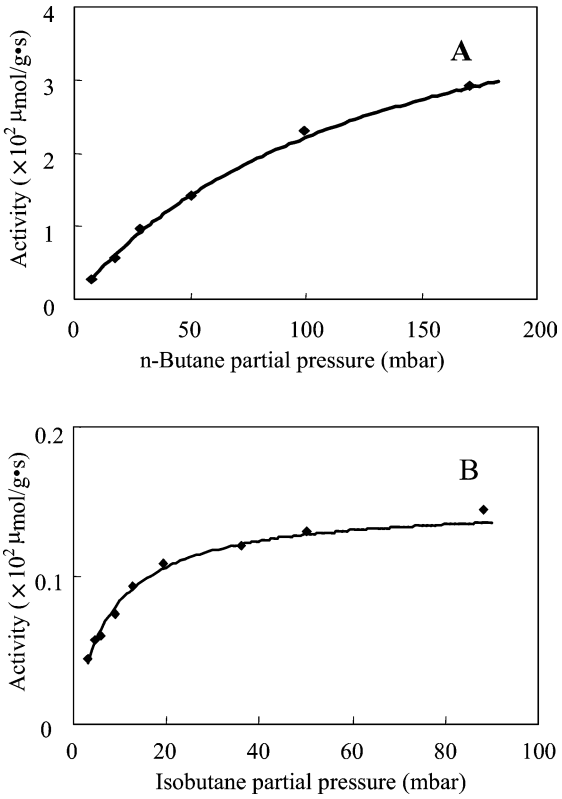

Fig. 8. (A) Experimental (◆) and predicated (—) isobutane formation rate versus *n*-butane partial pressure; and (B) experimental (◆) and predicated (—) *n*-butane formation rate versus isobutane partial pressure.

The second large true activation barrier found in the potential energy diagram of the reaction (see Fig. 9) is the hydride transfer (101 kJ/mol), obtained by analysis of the results of transient study with kinetic and transition-state theory. The close proximity of the values for the isomerization of the *sec*-butyl carbenium ion and the hydride transfer from *n*-butane to the *tert*-butyl carbenium ion suggests that limited room is available for improving the catalyst properties. This is related to the fact that the intramolecular isomerization and the hydride transfer require antagonistic properties of the catalyst. The isomerization rate is proportional to the stabilization of the cyclopropyl carbonium ion, which in-

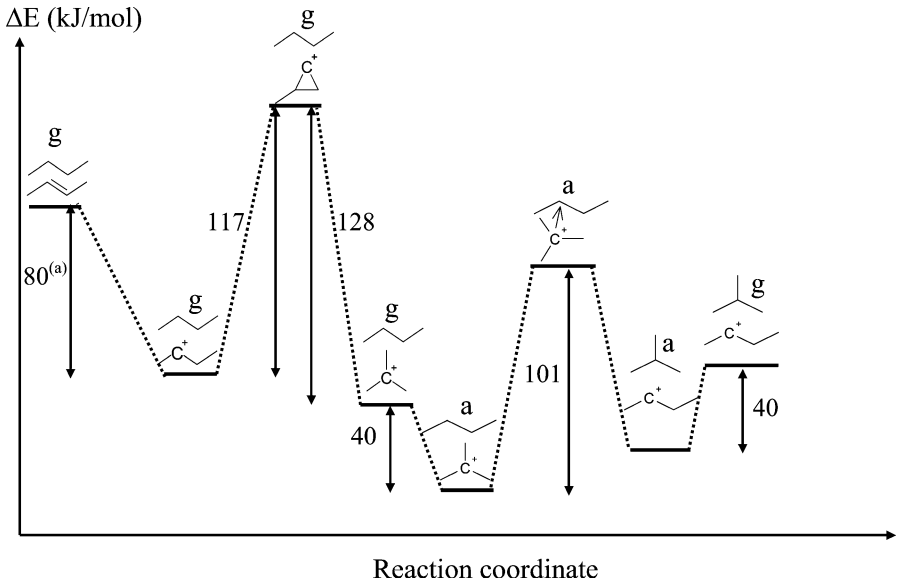

Fig. 9. Energy profile of isomerization/hydride transfer steps corresponding to isomerization of *n*-butane to isobutane. (a) Value taken from Yaluris et al. [27].

creases with increasing strength of the Brønsted acid sites. In contrast, the rate constant for hydride transfer from an alkane to an alkoxy group/carbenium ion increases with decreasing strength of the Brønsted acid sites [29]. Thus, the improvement of the isomerization would lead to a less favorable situation for the hydride transfer and eventually to the shift of the rate-determining step from the isomerization to the hydride transfer.

5. Conclusions

The isomerization is initiated by an oxidative dehydrogenation of *n*- and isobutane. Under differential conditions, the formed butene adsorbs on acid sites and isomerizes monomolecularly. The products are removed by hydride transfer.

Assuming approximately the same hydride transfer transition state for propane and *n*-butane, the transient experiments show that during *n*-butane isomerization more *n*- than isobutane can be removed by hydride transfer. This shows that more *sec*- than *tert*-butyl alkoxy groups/carbenium ions are present on the catalyst during isomerization. Because the most abundant reaction intermediate should be the one before the rate-determining step, we conclude that the isomerization of the carbenium ion is the rate-determining step in the chain sequence and that the hydride transfer is in quasi-equilibrium.

The variation of the yields in isobutane and in side products (propane and pentanes) with increasing conversion shows conclusively that isobutane is the only kinetically primary product of *n*-butane skeletal isomerization and that the side products are secondary products. Thus, main and side products are formed in sequential and not in parallel reactions. This is also confirmed by the high selectivity for isomerization for *n*- and isobutane at low conversion, which also implies that the isomerization occurs via an intramolecular mechanism. The true energies of activation (estimated by transition-state theory with the use of the experimentally determined thermodynamic and kinetic data) are 117 and 128 kJ/mol for the skeletal isomerization of the *sec*- and *tert*-butyl carbenium ion, respectively. This agrees well with the energetically demanding monomolecular reaction pathway.

The by-products, that is, propane and pentanes, are formed via bimolecular routes as secondary and tertiary products. At low to moderate conversions of *n*-butane, the relative concentrations of propane and pentane increase linearly with conversion. This is explained by the equilibrium between the *tert*-butyl carbenium ions and gas-phase isobutene. This isobutene alkylates carbenium ions at the surface, leading to octylcarbenium ions, which crack and undergo re-adsorption and hydride transfer. It is especially noteworthy that at higher conversion propane is formed almost exclusively, indicating that multiple alkylation and cracking steps occur under such conditions. Reversible isomerization and irreversible disproportionation are thus the cause of the reduced selectivity at high conversion in the absence of a hydrogenating function.

It is interesting to note that the forward rate of isobutane isomerization is significantly slower than the isomerization of *n*-butane, despite the fact that isobutane is easier to oxidize and is more stable as alkoxy groups/carbenium ions. This lower activity is associated with a higher energy of activation for the isomerization of the *tert*-butyl carbenium ion because of its higher stability compared with the *sec*-butyl carbenium ion. As a consequence, the difference in the methyl cyclopropyl carbonium ion and, hence, the true energy of activation are larger. The strong covalent bond of the carbenium ions in the ground state (alkoxy groups) leads,

however, to a dampening of the large differences expected from free carbenium ion chemistry.

The excellent fit of the kinetic model based on these conclusions shows that the reaction pathway for the isomerization of light *n*-alkanes on noble metal free sulfated zirconia can be outlined. Under differential conditions and at steady state the overall rate depends on the rate constant of the monomolecular isomerization of the carbenium ion, the concentration of the olefins in the catalyst zone, and the concentration of the Brønsted acid sites on the sulfated zirconia. The concentration of olefins in turn depends directly on the partial pressure of the alkane and the concentration of the labile sulfate-based redox sites of sulfated zirconia.

Acknowledgments

The financial support of the Deutsche Forschungsgemeinschaft (DFG) in the framework of the DFG priority program no. 1091, "Bridging the gap in Heterogeneous Catalysis," is gratefully acknowledged. We thank Prof. J. Sauer, Prof. H. Papp, Dr. F. Jentoft, Dr. C. Breitkopf, Dr. S. Wrabetz, Dr. K. Meinel, and Dr. A. Hofmann for fruitful discussions.

Appendix A

The propagation step of *n*-butane isomerization, hydride transfer, and skeletal isomerization of *sec*-butyl carbenium ion occurs many times (around 500) for each oxidation step. For the long-chain approximation, the formation and the termination rates of butene species are nearly identical:

$$k_{n1}[n\text{-}C_4H_{10}][SO_3] = k_{n5}[n\text{-}C_4H_8][T].$$

Thus, the steady-state concentration of *n*-butene is

$$[n\text{-}C_4H_8] = \frac{k_{n1}[SO_3][n\text{-}C_4H_{10}]}{k_{n5}[T]} = A'_n[n\text{-}C_4H_{10}],$$

were

$$A'_n = \frac{k_{n1}[SO_3]}{k_{n5}[T]}.$$

In a general treatment of the butene concentration, the differential equation of the residence time dependent olefin concentration in the reaction is

$$\frac{d[n\text{-}C_4H_8]}{dt} = k_{n1}[n\text{-}C_4H_{10}][SO_3] - k_{n5}[n\text{-}C_4H_8][T].$$

Solving this differential equation, we obtain the concentration of butenes:

$$[n\text{-}C_4H_8] = \frac{k_{n1}[SO_3][n\text{-}C_4H_{10}]}{k_{n5}[T]}\left(1 - e^{-k_{n5}[T]t}\right) = A''_n[n\text{-}C_4H_{10}],$$

where

$$A''_n = \frac{k_{n1}[SO_3]}{k_{n5}[T]}\left(1 - e^{-k_{n5}[T]t}\right).$$

Thus, if the termination rate is very fast, then

$$A''_n = \frac{k_{n1}[SO_3]}{k_{n5}[T]}\left(1 - e^{-k_{n5}[T]t}\right) = \frac{k_{n1}[SO_3]}{k_{n5}[T]} = A'_n$$

leading to the same solution as assumed in the steady-state approximation.

According to the mechanism proposed for *n*-butane skeletal isomerization on sulfated zirconia at low temperature, the differential equation describing the time dependent response of surface *sec*-butyl carbenium ion is

$$\begin{aligned}\frac{d[sec\text{-}C_4H_9^+]}{dt} &= k_{n2}[n\text{-}C_4H_8][H^+] - k_{n-2}[sec\text{-}C_4H_9^+] \\ &\quad - k_{n3}[sec\text{-}C_4H_9^+] + k_{n-3}[tert\text{-}C_4H_9^+] \\ &\quad + k_{n4}[tert\text{-}C_4H_9^+][n\text{-}C_4H_{10}] \\ &\quad - k_{n-4}[sec\text{-}C_4H_9^+][i\text{-}C_4H_{10}].\end{aligned}$$

With the pseudo-steady-state hypothesis $((d[sec\text{-}C_4H_9^+])/(dt) = 0)$, the concentration of *sec*-butyl carbenium ion can be described as

$$\begin{aligned}[sec\text{-}C_4H_9^+] = &\left(k_{n2}[n\text{-}C_4H_8][H^+] + k_{n-3}[tert\text{-}C_4H_9^+]\right. \\ &\left. + k_{n4}[tert\text{-}C_4H_9^+][n\text{-}C_4H_{10}]\right) \\ &\times \left(k_{n-2} + k_{n3} + k_{n-4}[i\text{-}C_4H_{10}]\right)^{-1}.\end{aligned}$$

Since at low conversion the concentrations of isobutane and *tert*-butyl carbenium ion during reaction are extremely low compared with *n*-butane and *sec*-carbenium ion, the description of concentration of *sec*-butyl carbenium ion can be simplified by the Most Abundant Surface Intermediates (MASI) assumption:

$$[sec\text{-}C_4H_9^+] = \frac{k_{n2}[n\text{-}C_4H_8][H^+]}{k_{n-2} + k_{n3}}.$$

From the site balance, carbenium ion and free Brønsted acid sites must be equal to the concentration of Brønsted acid sites, $[sec - C_4H_9^+] + [H^+] = C_B$, where C_B is the concentration of Brønsted acid sites and $[H^+]$ is the concentration of free Brønsted acid sites. Thus we can state that

$$[sec\text{-}C_4H_9^+] = \frac{C_B A_n[n\text{-}C_4H_8]}{1 + A_n[n\text{-}C_4H_8]},$$

where

$$A_n = \frac{k_{n2}}{k_{n-2} + k_{n3}}.$$

This shows that the concentration of *sec*-butyl carbenium ion is directly related to the concentration of butene species, which are formed by oxidation of *n*-butane by adsorbed SO_3 or pyro-sulfate species.

As we have concluded that the rate-determining step is the isomerization of the *sec*-butyl carbenium ion to the *tert*-butyl carbenium ion, the overall formation rate of isobutane normalized to the sample weight is

$$\frac{d[i\text{-}C_4H_{10}]}{dt} = r_n = k_{n3}[sec\text{-}C_4H_9^+].$$

Substituting for the [*sec*-$C_4H_9^+$], one obtains the rate equation in the simplest form:

$$r_n = \frac{k_{n3} C_B A_n A'_n [n\text{-}C_4H_{10}]}{1 + A_n A'_n [n\text{-}C_4H_{10}]}.$$

References

[1] X. Song, A. Sayari, Catal. Rev. Sci. Eng. 38 (1996) 329.
[2] G.D. Yadav, J.J. Nair, Micropor. Mesopor. Mater. 33 (1999) 1.
[3] K.B. Fogash, R.B. Larson, M.R. González, J.M. Kobe, J.A. Dumesic, J. Catal. 163 (1996) 138.
[4] H. Liu, V. Adeeva, G.D. Lei, W.M.H. Sachtler, J. Mol. Catal. A 100 (1995) 35.
[5] A.S. Zarkalis, C.Y. Hsu, B.C. Gates, Catal. Lett. 37 (1996) 1.
[6] A.S. Zarkalis, C.Y. Hsu, B.C. Gates, Catal. Lett. 29 (1994) 235.
[7] E.C. Sikabwe, R.L. White, Catal. Lett. 44 (1997) 177.
[8] V. Adeeva, H. Liu, B. Xu, W.M.H. Sachtler, Top. Catal. 6 (1998) 61.
[9] A. Sayari, Y. Yang, X. Song, J. Catal. 167 (1997) 346.
[10] X. Li, K. Nagaoka, L.J. Simon, R. Olindo, J.A. Lercher, A. Hofmann, J. Sauer (2004), submitted for publication.
[11] S. Hammache, J.G. Goodwin Jr., J. Catal. 211 (2002) 316.
[12] M.V. Luzgin, A.G. Stepanov, V.P. Shmachkova, N.S. Kotsarenko, J. Catal. 203 (2001) 273.
[13] V.B. Kazansky, Catal. Today 51 (1999) 419.
[14] H. Matsuhashi, H. Shibata, H. Nakamura, K. Arata, Appl. Catal. A 187 (1999) 99.
[15] V. Adeeva, G.D. Lei, W.M.H. Sachtler, Catal. Lett. 33 (1995) 135.
[16] F. Garin, L. Seyfried, P. Girard, G. Maire, A. Abdulsamad, J. Sommer, J. Catal. 151 (1995) 26.
[17] J. Sommer, R. Jost, M. Hachoumy, Catal. Today 38 (1997) 309.
[18] T. Echizen, T. Suzuki, Y. Kamiya, T. Okuhara, J. Mol. Catal. A: Chem. 209 (2004) 145.
[19] E. Garcia, M.A. Volpe, M.L. Ferreira, E. Rueda, J. Mol. Catal. A: Chem. 201 (2003) 263.
[20] M.V. Luzgin, S.S. Arzumanov, V.P. Shmachkova, N.S. Kotsarenko, V.A. Rogov, A.G. Stepanov, J. Catal. 220 (2003) 233.
[21] Z. Ma, W. Hua, Y. Ren, H. He, Z. Gao, Appl. Catal. A: Gen. 256 (2003) 243.
[22] S.Y. Kim, J.G. Goodwin Jr., D. Fărcaşiu, Appl. Catal. A: Gen. 207 (2001) 281.
[23] A. Sassi, J. Sommer, Appl. Catal. A 188 (1999) 155.
[24] M.J. Cleveland, C.D. Gosling, J. Utley, J.E. Elstein, NPRA Annual Meeting, 1999.
[25] M. Boronat, P. Viruela, A. Corma, J. Phys. Chem. 100 (1996) 633.
[26] M.V. Frash, R.A. van Santen, Top. Catal. 9 (1999) 191.
[27] G. Yaluris, J.E. Rekoske, L.M. Aparicio, R.J. Madon, J.A. Dumesic, J. Catal. 153 (1995) 54.
[28] A.M. Rigby, G.J. Kramer, R.A. van Santen, J. Catal. 170 (1997) 1.
[29] A. Feller, A. Guzman, I. Zuazo, J.A. Lercher, J. Catal. 224 (2004) 80.